Appl. Phys. A 74, 773–777 (2002)/ Digital Object Identifier (DOI) 10.1007/s003390100943

Applied Physics A
Materials
Science & Processing

Micromachining of complex channel systems in 3D quartz substrates using Q-switched Nd:YAG laser

S.-J. Qin, W.J. Li*

Center for Micro and Nano Systems, The Chinese University of Hong Kong, Hong Kong

Received: 15 January 2001/Accepted: 5 June 2001/Published online: 30 October 2001 – © Springer-Verlag 2001

Abstract. A novel microchannel fabrication technology for quartz using a Q-switched Nd:YAG laser is presented. Complex 3D channel systems inside quartz substrates can be constructed directly using a laser beam by controlled fracturing, and high-quality microchannels can be fabricated by melting quartz using a laser-induced plasma. The behavior of laser-induced plasmas in drilling microchannels is discussed. The diameter of the microchannels can be controlled from 25 to 200 μm. The average roughness of the interior channel wall is less than 0.2 μm. Currently, microchannels longer than 4 mm in fused-quartz cubes can be achieved using laser-induced plasmas.

PACS: 42.60; 81.40

Many microchannel systems, which are used to improve performance and add new functionality in many applications such as chemical, blood, DNA, and environmental science analyses, are typically fabricated on quartz or silicon substrates. Quartz is sometimes more suitable than silicon for these purposes because it is (1) optically transparent, (2) chemically inert and stable, (3) a good electrical insulator, and (4) cheaper than silicon. Also, quartz substrates with a wide range of dimensions are available. However, almost all quartz micromachining for these systems is performed by conventional IC or MEMS technologies such as lithography and etching [1, 2]. These conventional technologies have many limitations on fabrication, bonding, and packaging of a final system.

Recently, much attention has been paid to Q-switched Nd:YAG laser micromachining for MEMS/microsystems applications due to a number of advantages: it is a single-step process with high flexibility, and relatively high resolution. There are two major difficulties in using a Q-switched Nd:YAG laser to machine quartz. First, quartz is an optically transparent material and its average absorptivity for the spectrum from visible to near infrared is less than 5%. For this reason there are few reports about micromachining on quartz directly using Nd:YAG lasers, since very high laser power is required to process these substrates. The second problem is the typical strong thermal effect induced in materials by laser ablation using standard nanosecond (ns) lasers. This effect may cause severe damage and cracks in hard and brittle materials, e.g. quartz. Nevertheless, a few research groups have recently developed novel techniques to micromachine quartz using lasers. Gratings on a quartz substrate surface were etched using a Nd^{+}:YAG laser (266 nm) by laser-induced plasma-assisted ablation [3, 4]. Well-defined and highly reproducible straight microchannels were fabricated in quartz using ultrashort (100–200 fs) laser pulses. The channels were of a few μm in diameter with lengths over 1 mm [5]. A comprehensive comparison of the quality of the laser-ablated channels using fs, ps, and ns pulse lengths was also given in [5], which showed that the main parameter influencing the quality of the laser ablation is laser pulse length. A related research group later showed that self-focusing of ps laser pulses due to the nonlinear Kerr effect can be used to produce microstructures in quartz substrates without damaging the entrance or exit surfaces of the substrates [6]. However, none of these works has demonstrated straight microchannels that are more than 2 mm in length, and they have not investigated the channel interior-wall quality as a function of different laser machining processes.

We will describe our current work in using a Nd:YAG laser beam (1064 nm) to directly create complex microchannel systems bounded by solid 3D quartz substrates of any shape by means of special laser micromachining processes. We have shown that straight and bent microchannel systems much longer than those demonstrated in [3–6] can be fabricated by both thermal-induced and plasma-induced laser machining. The effect of these processes on the channel interior wall roughness was also investigated. Furthermore, we have found that channel diameters can be controlled by varying the laser drilling patterns.

The physical principle that allowed us to process optically transparent quartz cubes is the so-called electric breakdown effect of the electric field [7]. Based on the effect, the electric field strength at the exit surface can be higher than the electric field strength at the laser beam entrance surface. This is due to

*Corresponding author. (E-mail: wen@acae.cuhk.edu.hk)

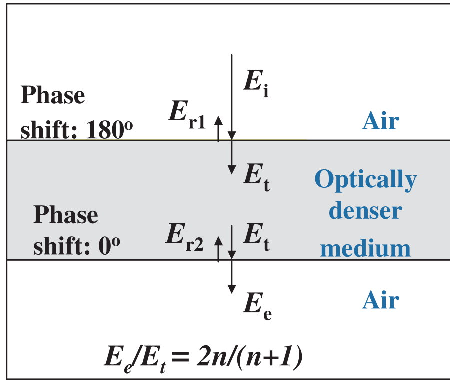

Fig. 1. Illustration of transmitted and reflected amplitude of a light beam incident on an air-medium interface

the fact that when a light beam passes from an optically less dense medium to a denser one, there will be 180° phase shift at the entrance surface but no phase shift at the exit surface for the reflected beam (see Fig. 1). The ratio of electric field strength at the exit (E_e) and the entrance (E_t) surfaces can be calculated as:

$$\frac{E_e}{E_t} = \frac{2n}{n+1} \tag{1}$$

where n is the refractive index of the medium.

If the material refractive index is 1.5, e.g. as for quartz, the ratio of electric field strength at the exit and entrance surfaces E_e/E_t is 1.2 and the ratio of laser intensity at both surfaces is

$$\frac{I_e}{I_t} = \left(\frac{E_e}{E_t}\right)^2 = 1.44 \tag{2}$$

So, it is easier to process quartz from the rear surface of substrates. As soon as the first laser pulse drilling occurred at the back surface, the locally damaged site can absorb thermal energy from the following pulses, and thermal-induced or plasma-induced laser processing can be initiated from the site. Hence, microchannels can be formed in any part of the quartz by defining paths starting from this site.

1 Experimental

A Q-switched Nd:YAG laser, with 40 W maximum power (Electrox Scriba II D40, UK), was used in our work. The frequency of the laser pulse was set at 2 kHz and the pulse width of the laser was 100–300 ns. The laser beam was focused by a scanning lens (f·θ lens) with a focal length of 100 mm onto the sample surface. The Gaussian spot size of the beam was determined to be about 400 μm^2 at 1064 nm (radius of $\sim$ 11.3 μm at $1/e^2$ intensity). All channels were formed in optical-grade fused-quartz cubes (bubble-free synthetic silica, Almaz Optics, Inc., USA). The drilling processes were carried out in air with atmospheric pressure with the laser beam directly focused on the substrates (maskless).

Two methods for laser drilling on quartz were studied in our work: laser-controlled fracturing and laser melting. Laser drilling by controlled thermal fracturing can usually be accomplished with relatively low power (on the order of 100 W or less) so the Nd:YAG laser beam may be used directly to perform drilling, which we will refer to as thermal-induced processing. However, laser drilling on quartz by melting usually requires laser powers above 1000 W even with CO_2 lasers [8]. We have used laser-induced plasmas at extremely high temperature to process quartz with our 40-W laser system, which we refer to as plasma-induced processing. Both technologies are able to construct microchannels in solid 3D quartz substrates, and the latter tends to create better channels.

2 Results and discussion

2.1 *Laser-controlled fracturing*

A microscope photo of a channel fabricated by thermal-induced processing is shown in Fig. 2. By knowing the laser pulse frequency, pulse width, focal spot, and measured average power, the laser fluence at the rear surface of the sample was estimated to be about 160–370 J/cm^2 (0.65–1.5 mJ pulse energy) for the thermal-induced process. The average laser power was measured using a Power MAX5200 laser power meter (Molectron, Detector Inc.). Since the energy of the laser was not high enough to melt the quartz in this process, the channels were formed mainly through thermal cracking. Quartz is a fragile material, so the channel shape depends strongly on the state of stress of the quartz during the laser

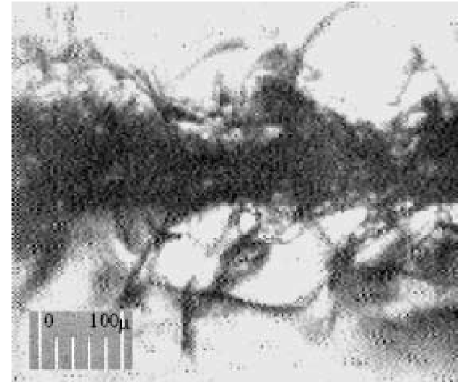

Fig. 2. A microscope photo of micro-channel drilled by thermal-induced processing with many thermal cracks

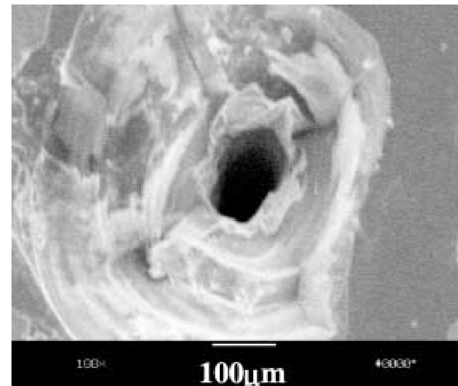

Fig. 3. SEM picture of the cross-sectional view of a channel drilled by thermal-induced processing

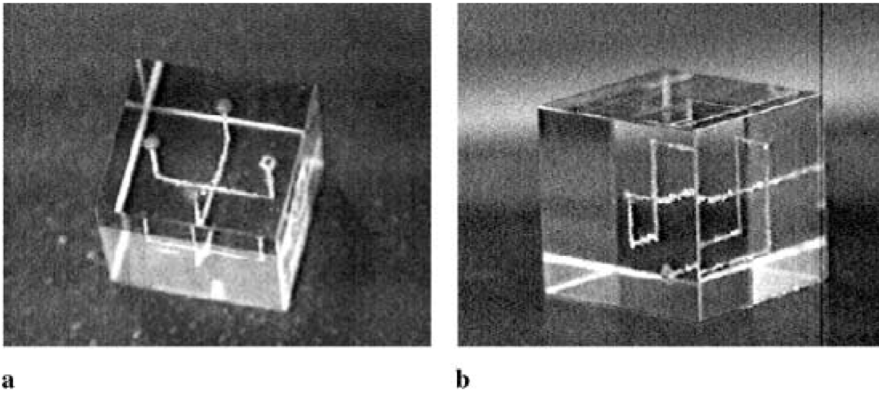

Fig. 4a,b. Photos of different channel systems in 3D quartz cubes of $10 \times 10 \times 10\ mm^3$: **a** a fluidic mixer consisting of two U-shape channels with the length of 2×21 mm, **b** a more complex 3D channel system with total channel length of 34 mm

interaction. As shown, there are many thermal cracks around the channel. Also, residual stresses in the quartz may cause secondary fracturing. This effect affects the channel cross-section and reduces the straightness of the channel. The channel cross-sectional geometry cannot be well controlled, as shown in Fig. 3.

It is possible to adjust the incoming laser field strength such that the threshold energy needed to locally damage the quartz, is reached at the exit surface or at an existing erosion front inside a quartz substrate and not the entrance surface, so laser processing can only occur on a defined path without damaging the surface and any other area, even though the laser beam passes through them. Two channels in different directions can be connected easily by this method. Based on the connection of channels in two directions, complex 3D channel paths inside the quartz cube can be constructed. Figure 4 shows photos of different microchannel systems in 3D quartz cubes with dimensions of 10 mm × 10 mm × 10 mm.

2.2 Laser melting

The thermal cracks around the channels may be reduced or eliminated by locally melting the quartz instantaneously. A laser-induced plasma of quartz was used to perform drilling by melting. Re-solidified molten quartz may produce smooth and clean channel wall surfaces.

Plasma of most elements can be produced by a high-intensity pulsed-laser irradiation. When a series of laser pulses strike a solid target and are absorbed by the target, a characteristic sequence of energy conversion processes leads to the production of hot and dense plasma consisting of matter in an extreme state of high-energy concentration [9]. The structure of the solid target plays a key role during the laser-target interaction. A flat target may just absorb incoming irradiation once, whereas a cavity may store irradiation for a much longer time by reflecting the irradiation on the interior wall of the cavity. Therefore, there is much more opportunity for a cavern target to absorb irradiation energy and a plasma may be more easily induced in a cavity.

A quartz substrate was first pre-damaged at a site by thermal-induced processing, and the following laser pulses could be easily absorbed by this locally damaged site. Then the laser beam was focused on this initiated site on the quartz surface. Once the damaged site began to absorb enough laser energy, a hot and dense plasma of quartz was produced around this site. The plasma attacked and melted the neighboring quartz and then a hollow was formed. The hollow functioned as a cavity for the following laser pulses. The laser-induced plasma of quartz was produced in the cavity on each subsequent pulse to drill the hollow further downward, producing a microchannel. The channels fabricated by this process are of high quality with a smooth kerf surface and no thermal cracks are observed, as shown in Fig. 5.

2.3 Analysis of the drilling processes

The behavior of both thermal-induced processing and plasma-induced processing were studied and are discussed below. Figure 6 shows SEM pictures of channels processed by a laser-induced plasma, indicating that the channels were

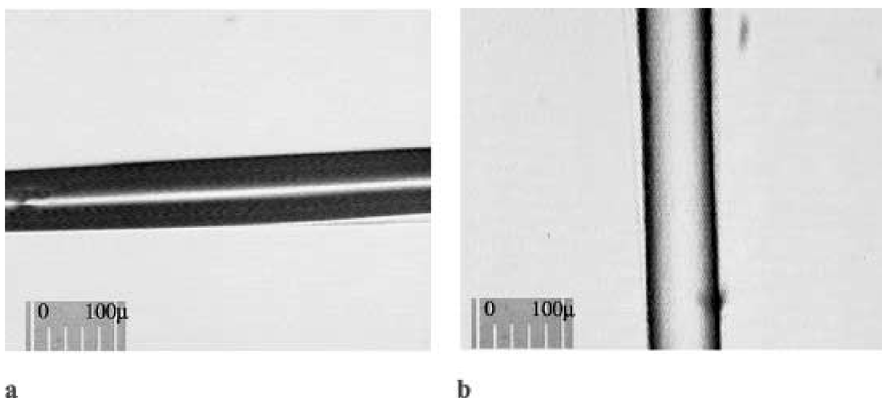

Fig. 5. Microscope photos of microchannels with clean kerf surface drilled by laser-induced plasma. **a** A channel before filling in electrolyte. **b** A channel after filling in electrolyte $FeCl_3$

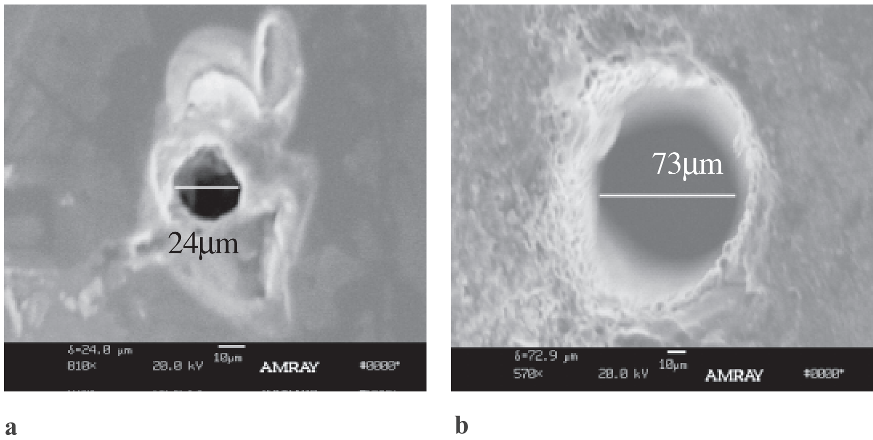

Fig. 6a,b. SEM pictures of channels drilled by laser-induced plasma with different diameters: **a** 24 µm, **b** 73 µm

basically circular in shape. The laser fluence at the sample surface is estimated to be about 320–620 J/cm^2 (1.3–2.5 mJ pulse energy) in plasma-induced processing (laser fluence was estimated using the same method discussed in Sect. 2.1).

In order to control the dimension of the channels, the laser beam was moved in different drilling patterns instead of just focusing on one spot on the cutting plane. The diameter of the channels can be varied from around 25 to 200 µm by controlling the laser beam to move in circular patterns with different radius. In our experiment, we have tried both cross patterns and circular patterns when implementing the thermal-induced processing. The latter tends to produce larger thermal cracks and could directly control the dimensions of the channels. The former may produce smaller thermal cracks but could not be used to control the channel dimensions. In the plasma-induced processing, one-circle or multi-circle patterns were used and the latter tend to create more uniform channels. Figure 7 shows the dependence of the channel diameter on the dimension of the circular drilling pattern for the thermal-induced processing.

Fig. 8 shows a SEM picture of the interior wall of a channel drilled by a laser-induced plasma, indicating that smooth interior walls can be produced by laser-induced plasmas. The quantitative analysis on the roughness of interior wall was

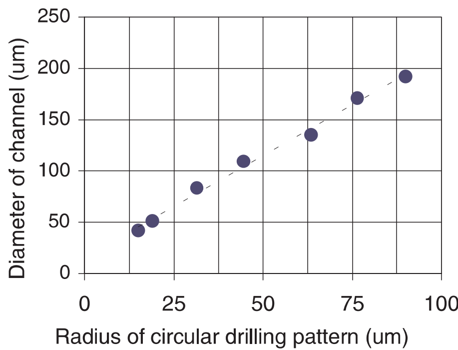

Fig. 7. The dependence of channel diameter on the dimension of circular laser drilling pattern in thermal-induced processing

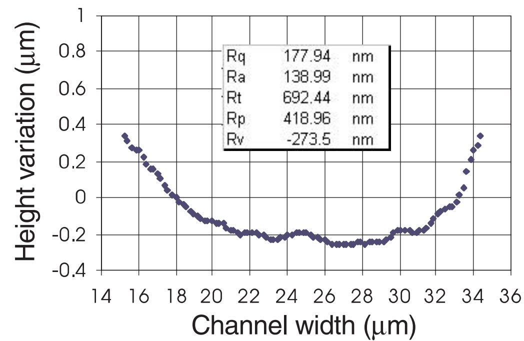

Fig. 9. WYKO interferometer plot of the channel interior surface. The parameters, R_q, R_a, R_t, R_p, and R_v , are root mean square roughness, roughness average, maximum height of the profile, maximum profile peak height, and maximum profile valley depth, respectively

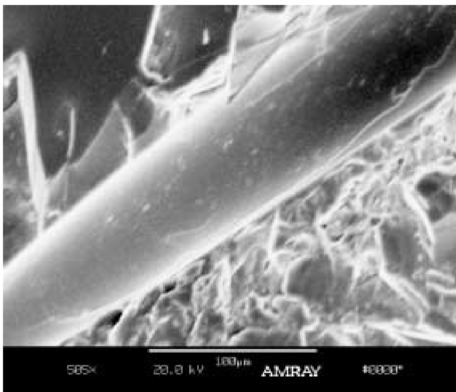

Fig. 8. SEM picture of channel interior wall drilled by laser-induced plasma

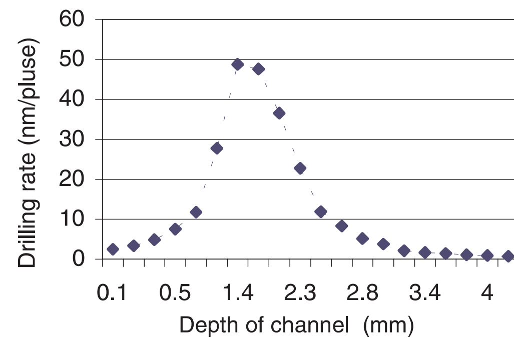

Fig. 10. The dependence of drilling rate on depth of hole for a channel of ∼ 80 µm in diameter (at laser fluence: 620 J/cm^2, frequency: 2 kHz, pulse width: 200 ns)

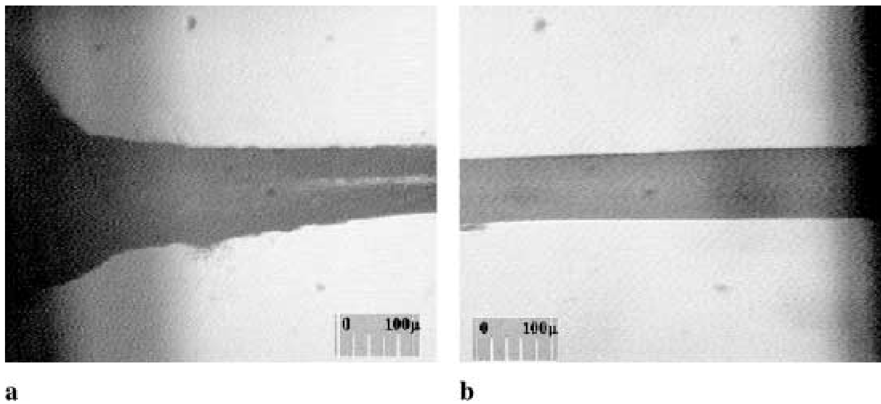

Fig. 11a,b. Microscopephotos of a through channel on a 4-mm-thick fused quartz substrate. **a** The beginning part of channel. **b** The end part of channel

carried out using the WYKO Surface Profiler and the result is shown in Fig. 9, indicating that the roughness average, *Ra*, is less than 0.2 μm for the channel measured.

The plasma density changed with the depth of hole as well as the laser intensity so that the drilling rate varied with the depth of hole, as shown in Fig. 10. The drilling rate behavior can possibly be explained by dividing the process into three stages: beginning, middle, and end. At the beginning stage, just before the hole was formed, the quartz cube was a flat target for the incident laser beam. The laser-induced plasma of quartz was produced only when the quartz target absorbed enough laser energy at the pre-damaged site. The quartz plasma with high temperature melted and vaporized the quartz exposed to the incident beam, forming a hole. At the middle stage, as the depth of hole increased, the hole functioned as a cavity. The laser beam might bounce in it several times, providing more opportunities for the quartz target to absorb irradiation energy and induce a hot and dense plasma of quartz. During this stage, the quartz plasma was of the highest temperature and density, giving the fastest drilling rate in the whole drilling processes. The depth of hole in this stage was about 0.5 mm to 2.5 mm. At the end stage, as the hole got deeper, the laser irradiation might heat the air in the cavity as well as the quartz target, inducing both quartz plasma and air plasma. The front air plasma with a high dielectric constant is of high absorptivity to the laser beam, and can shield part or all of the subsequent laser pulses to reach the quartz target. In this stage the mixture of both plasmas was gradually weakened and therefore the drilling rate was gradually decreased until zero.

We have successfully fabricated microchannels longer than 4 mm on quartz cubes with dimensions of 10 mm × 10 mm × 10 mm by laser-induced plasma. Figure 11 shows the beginning part and the end part of a through channel on a quartz substrate. Note that the quartz plasma is more easily induced at the beginning part of a channel, leading to larger openings (see Fig. 11a). At the end stage of drilling a blind hole on a thick cube, the diameter of channel might decrease as the plasma weakens, forming a nozzle shape. However, once a through channel was formed, the laser beam would be incident on the base-plate material under the quartz substrate (aluminum plate was used in our experiment), and then induced aluminum plasma, by which the end part of channel can be re-drilled, producing a uniform channel, as shown in Fig. 11b.

3 Conclusion

A new method for high-quality microchannel fabrication is presented. This technology not only allows the rapid construction of complex 3D channel paths inside a quartz cube by thermal-induced laser processing, but also creates high-quality microchannels with lengths longer than 4 mm using laser-induced plasma. The application of these microchannels to fluidic devices is being investigated. This new technology will enable flexible and fast fabrication of various kinds of 3D microfluidic systems such as micro mixers, micro pumps, capillary electrophoresis (CE) systems, and micro total analyses systems (μTAS), and lead to new applications of MEMS in biomedical engineering.

Acknowledgements. We would like to thank the Solid State Electronics Lab in the Department of Electronic Engineering, CUHK, for the SEM pictures taken in this project. We also deeply appreciate Dr. Xia Yunjie for his helpful discussion.

References

1. T. Kikuchi, T. Ujiie, T. Ichiki, Y. Horiike: *Microprocesses and Nanotechnology '99 International*, 178 (1999)
2. H. Nakanishi, T. Nishimoto, N. Nakamura, S. Nagamachi, A. Arai, Y. Iwata, Y. Mito: Micro Electro Mechanical Systems MEMS'97, Proc. IEEE., 10th International Workshop, 299 (1997)
3. J. Zhang, K. Sugioka, K. Midorikawa: Appl. Phys. A **67**, 545 (1998)
4. J. Zhang, K. Sugioka, K. Midorikawa: Appl. Phys. A **69**, 879 (1999)
5. H. Varel, D. Ashkenasi, A. Rosenfeld, M. Wahmer, E.E.B. Campbell: Appl. Phys. A **65**, 367 (1997)
6. D. Ashkenasi, H. Varel, A. Rosenfeld, S. Henz, J. Herrmann, E.E.B. Campbell: Appl. Phys. Lett. **72**, 1442 (1998)
7. C.J. Nonhof: *Material Processing With Nd-lasers* (Electrochemical Publications, Ayr, UK 1988) p. 246
8. K. Yamazaki, H. Kanenatsu: Proc. Laser Advanced Materials Processing, International, 208 (1987)
9. A. Rubenchik, S. Witkowski: *Physics of Laser Plasma* (North-Holland, Amsterdam, London 1991) p. 64